Key Points:
- New method to calculate groundwater compressible storage from the response of hydraulic heads to tidal drivers at subdiel frequencies
- Comparing three contrasting barometric efficiency results with traditional correlation plots illustrates the superiority of the new method
- The new method is simple, accurate, and only uses commonly available measurements of atmospheric pressure and groundwater head

Correspondence to:
R. I. Acworth,
i.acworth@unsw.edu.au

An objective frequency domain method for quantifying confined aquifer compressible storage using Earth and atmospheric tides

R. Ian Acworth[1,2], Landon J. S. Halloran[1,2], Gabriel C. Rau[1,2], Mark O. Cuthbert[1,3], and Tony L. Bernardi[4,5]

[1]Connected Waters Initiative Research Centre, School of Civil and Environmental Engineering, UNSW Australia, Sydney, New South Wales, Australia, [2]Water Research Laboratory, School of Civil and Environmental Engineering, UNSW Australia, Sydney, New South Wales, Australia, [3]Department of Geography, University College London, London, UK, [4]NSW Department of Primary Industries, Orange Agricultural Institute, Orange, New South Wales, Australia, [5]Dryland Salinity Hazard Mitigation Program, Institute for Applied Ecology, University of Canberra, Canberra, Australian Capital Territory, Australia

Abstract The groundwater hydraulic head response to the worldwide and ubiquitous atmospheric tide at 2 cycles per day (cpd) is a direct function of confined aquifer compressible storage. The ratio of the responses of hydraulic head to the atmospheric pressure change is a measure of aquifer barometric efficiency, from which formation compressibility and aquifer specific storage can be determined in situ rather than resorting to laboratory or aquifer pumping tests. The Earth tide also impacts the hydraulic head response at the same frequency, and a method is developed here to quantify and remove this interference. As a result, the barometric efficiency can be routinely calculated from 6-hourly hydraulic head, atmospheric pressure, and modeled Earth tide records where available for a minimum of 15 days duration. This new approach will be of critical importance in assessing worldwide problems of land subsidence or groundwater resource evaluation that both occur due to groundwater abstraction.

1. Introduction

The calculation of the barometric efficiency (BE) from changes in groundwater head and atmospheric pressure has been extensively discussed in the past [*Hsieh et al.*, 1987; *Rojstaczer and Agnew*, 1989; *Acworth and Brain*, 2008]. If porosity data are available or can be estimated and the BE is known, then the groundwater specific storage and formation compressibility can also be quantified [*Domenico and Schwartz*, 1997]. Accurate estimates of specific storage are important for groundwater modeling, and the aquifer compressibility is of paramount significance in the estimation of land subsidence. Alongside, ever increasing groundwater extraction due to population growth [*Wada et al.*, 2010] and climatic cycles [*Alley et al.*, 2002], land subsidence is a major global problem [*Galloway and Burbey*, 2011; *Higgins et al.*, 2013].

The initial concept proposed by *Jacob* [1940] was that a change in groundwater head measured in a piezometer was directly proportional to the change in atmospheric pressure. The constant of proportionality was referred to as the BE. BE=0 for an unconfined aquifer in which, by definition, the water table occurs where the water pressure is equal to the atmospheric pressure.

For situations where extensive low hydraulic conductivity material exists between water and the surface, the (ground) water becomes confined and only a portion of the change in atmospheric pressure is transmitted to the water pressure. In the limit that the material has a formation compressibility significantly smaller than the water compressibility, all the stress change due to a change in atmospheric pressure is accommodated by the formation. In this situation, the hydraulic head measured in the piezometer is equivalent to a (negative) barometer and the BE = 1. A decrease in atmospheric pressure results in an instantaneous increase in the hydraulic head, and importantly, the movement of hydraulic head should be exactly out of phase with the change in atmospheric pressure. As the structural integrity of the material reduces (i.e., compressibility increases), a proportion of the stress change is carried by the water and the total stress change is partitioned between the formation and the water. Under these conditions, BE< 1.

Of particular interest is the fact that the spectra of atmospheric pressure records contain clear amplitude peaks at exactly 1 and 2 cpd (cycles per day). These signals have a smaller amplitude than the lower frequency mesoscale processes that impact atmospheric pressure. However, although smaller in amplitude, their frequency is very stable when compared to the mesoscale components. *Palumbo* [1998] has shown that the cause of these peaks in atmospheric pressure is due to interference between the diel variation in pressure through the atmosphere related to changes in air temperature and pressure as the Earth rotates. The 2 cpd atmospheric pressure oscillation, first observed by *Jean Honoré Robert de Paul de Lamanon* in 1785 [*Cartwright*, 1999], is a reliable and worldwide phenomenon that causes a response in hydraulic heads [*Merritt*, 2004] and even variations in surface discharge of inland rivers [*Briciu*, 2014].

The identification of Earth tides [*Merritt*, 2004; *Cutillo and Bredehoeft*, 2011] and the spectral complexity of the atmospheric tide [*Palumbo*, 1998] complicate analysis of the hydraulic head response to atmospheric tides. Five components contribute approximately 95% of the Earth tides. These frequencies occur at 0.9295 cpd (O_1: Principal lunar); 1.0029 cpd (K_1: Lunar solar); 1.9324 cpd (M_2: Principal lunar); 2.0000 cpd (S_2: Principal solar), and 1.89957 cpd (N_2: Lunar elliptic) [*Cutillo and Bredehoeft*, 2011]. It is noted that the Lunar solar and the Principal solar components of the Earth tide occur at the same frequencies as the atmospheric tides.

Cutillo and Bredehoeft [2011] used the Earth tide frequencies that are independent of the atmospheric tide, observing that the K_1 and S_2 components of the Earth tide are contaminated by the atmospheric pressure variation. They concentrated on the O_1 and M_2 components of the Earth tide in their analysis of aquifer properties.

In this paper we develop a new frequency domain method for the exact calculation of aquifer BE by disentangling the combined atmospheric and Earth tide influence on the amplitude response of hydraulic heads at 2 cpd (S_2). To demonstrate the usefulness of the new method, we calculate the groundwater compressible storage properties at three locations with contrasting conditions ($0 < BE < 1$).

2. Methodology

2.1. Relationships Between Groundwater Compressible Storage Properties

We assume that undrained conditions apply for hydraulic head oscillations at subdiel frequencies ($1 < f < 2$ cpd) [*Rojstaczer*, 1988; *Rojstaczer and Agnew*, 1989] and recognize that [*Jacob*, 1940; *Van Der Kamp and Gale*, 1983]

$$BE = 1 - \gamma, \tag{1}$$

where γ is the loading efficiency (−). This loading efficiency can be expressed as the ratio of terms involving compressibility

$$\gamma = \frac{\alpha}{\theta\beta + \alpha}, \tag{2}$$

where α is the formation compressibility (Pa^{-1}), and β is the fluid compressibility (Pa^{-1}) (4.59×10^{-10} Pa^{-1} at 20°C), and θ is the aquifer porosity (−). With α, β, and θ either known or assumed, the value of specific storage (m^{-1}) for the confined formation is [*Cooper*, 1966]:

$$S_s = \rho g \left(\alpha + \theta\beta \right). \tag{3}$$

2.2. Barometric Efficiency Calculated From Tidal Amplitudes

In this paper we use the tide acronyms by *Merritt* [2004] and *Cutillo and Bredehoeft* [2011] to identify the different frequency components. We add the superscripts GW for groundwater (hydraulic head), ET for Earth tides, and AT for atmospheric tides. While the hydraulic head responds to both the atmospheric pressure variation at 1 and 2 cpd, *Acworth and Brain* [2008] noted that there was significant seasonal amplitude variation in the 1 cpd signal and suggested only using the 2 cpd signal. We also note that it was for this reason that *Cutillo and Bredehoeft* [2011] rejected using either the 1 cpd signal or 2 cpd and concentrated their analysis on the Earth tides at frequencies of 0.9295 cpd (O_1) and 1.9324 cpd (M_2).

To better understand the time variability of the 1 cpd and 2 cpd atmospheric signals, we used the wavelet synchrosqueezed transform (WSST) method to map the time-frequency-amplitude content [*Daubechies et al.*, 2011]. WSST significantly "sharpens" the frequency-time resolution compared to the continuous

wavelet transform. Based on the original WSST, *Thakur et al.* [2013] developed a version for discrete data which is now officially implemented in *MATLAB*® (release R2016a).

Acworth and Brain [2008] illustrated a way to utilize the amplitude of subdiel frequency components contained in hydraulic heads in order to calculate BE. Their method relies on the fact that only Earth tide influences are present at a frequency of 1.9324 cpd (M_2^{ET}), whereas both Earth tide and barometric effects are contained in the groundwater response at 2 cpd (S_2^{GW}). To separate the two drivers in S_2^{GW}, they recognized that the ratio of the Earth tides S_2^{ET}/M_2^{ET} will be constant and that, as M_2^{GW} is uncontaminated by the atmospheric signal, the value of the Earth tide component in S_2^{GW} could be predicted by multiplying M_2^{GW} by S_2^{ET}/M_2^{ET}.

However, *Acworth and Brain* [2008] neglected the fact that when two harmonic signals with the same frequency are superimposed, for example, the 2 cpd component of Earth tide S_2^{ET} and atmospheric tide S_2^{AT}, the result is a new harmonic at the same frequency but with a different amplitude and phase (*Harmonic Addition Theorem*). In other words, components of drivers with the same frequency but differing amplitudes and phases simultaneously act to cause groundwater oscillations with predictable amplitude and phase.

To accurately quantify how much of each component is contained in the groundwater head and to determine the exact correction to apply to S_2^{ET}, the amplitude of the Earth tide must be corrected using the phase difference between the atmospheric tide S_2^{AT} and the Earth tide M_2^{ET}. This results in

$$\text{BE} = \frac{S_2^{GW} + S_2^{ET}\cos(\Delta\phi)\frac{M_2^{GW}}{M_2^{ET}}}{S_2^{AT}}, \tag{4}$$

where $\Delta\phi$ is the phase difference (rad) between the Earth tide and atmospheric drivers, S_2^{ET} and S_2^{AT}. The direction of the phase shift is inconsequential because of the *cosine* function's symmetry about 0. The amplitude correction ($S_2^{ET}\cos(\Delta\phi)\frac{M_2^{GW}}{M_2^{ET}}$) is mathematically added as the groundwater response is out of phase by exactly 180° (or π radians) compared to the atmospheric driver S_2^{AT}.

Equation (4) can be combined with equations (1)–(3) to calculate groundwater compressible storage using the subdiurnal frequencies as a natural tracer. For example, the formation compressibility can be quantified through equations (1) and (2), or the specific storage through equations (1) and (3).

2.3. Spectral Estimation of Component Amplitudes and Phases

The determination of the amplitudes and phases of relevant components from a signal $s(t)$ with sampling rate f_s is accomplished via the discrete Fourier transform, $\mathcal{F}$, as implemented in the *Fast Fourier Transform* (FFT). The frequencies of the two signals of interest, M_2 and S_2, are accurately known, and the data set may be of any length greater than ∼15 days, although we assume that there are an even number of evenly spaced samples per day.

The amplitude and phase information are determined using two different approaches. For the phase information, only the M_2 phase is of interest, thus allowing for unfiltered treatment of the data. First, the record of interest is cut so that its total duration of N samples is a multiple of 12 h (i.e., the period of the S_2 component). The Fourier transform of this signal is

$$\hat{s}(f_k) = \mathcal{F}\{s(t_n)\} = \sum_{n=0}^{N-1} s(t_n)e^{-2\pi ikn/N} \tag{5}$$

where k and n denote the indices of discretely sampled frequency and time, respectively, which range from 0 to $N-1$. Here normalization of the transform is unimportant as long as one is consistent across data sets because only ratios of amplitudes are used in the calculation method. The discrete frequencies of the transformed signal are

$$f_k = kf_s/N. \tag{6}$$

The phase, ϕ, of the M_2 component can therefore be calculated from the complex value of the FFT of the signal at index $k = Nf_{M2}/f_s$, which, due to the signal duration being truncated to an even multiple of the M_2 period, is an integer.

FFT analysis allows investigation of the phase lags between the various components of a signal, and it is possible using FFT implementations in various programming languages (e.g., MATLAB®; Python, or R) or by other software such as TSoft [*Van Camp and Vauterin*, 2005].

To resolve the amplitudes of the M_2 and S_2 components, a similar FFT-based technique is performed. A *Hanning* window [*Harris*, 1978] of the same length as the input signal is applied to the entire signal as a vector dot product in order to minimize spectral leakage. The result is then padded with the average value of the signal so that the padded signal length is equal to a power of 2.

2.4. Barometric Efficiency Estimation Using Time-Domain Correlation

Gonthier [2007] and *Acworth and Brain* [2008], working in the time domain, constructed scatterplots of all the atmospheric and hydraulic head data available at a field site. If there is a significant BE apparent in the data, it can be deduced from sequences of data that plot with a linear tendency (i.e., BE equals the slope of this correlation plot).

The method performs well for very high BE values where the aquifer is not impacted by other processes (e.g., recharge or extraction). In this instance, a linear fit to the data will give a slope that is the BE. For data sets impacted by modification of groundwater storage, other factors obscure the simple linear relationship. Here we compare these hydraulic head versus atmospheric pressure plots with our new frequency domain-based results.

2.5. Field Sites, Pressure Monitoring, and Earth Tide Synthesis

To demonstrate the new method, records for three different field sites in Australia are used.

1. Baldry, NSW, Australia (Borehole BH1: latitude −32.868088°, longitude 148.536771°) where groundwater heads have been monitored by various vented level sensors over the 12 year period. Atmospheric pressure was monitored by an absolute gauge transducer (Vaisala, Finland). The data for this analysis were from a peizometer (BH1) completed at 20 m depth in fractured rock below a confining layer of silt [*Acworth and Brain*, 2008].
2. Cattle Lane, NSW, Australia (Piezometer P35: latitude −31.518340°, longitude 150.468332°) where hydraulic heads have been monitored using a vented transducer (Level Troll 700H series, In-Situ Inc., USA) and atmospheric pressure measured by an absolute gauge transducer (Baro Troll, In-Situ Inc., USA). A succession of silts and clays overlies this piezometer screened at 35 m depth in a sandy silty clay. This succession has been proven by taking a core to 31 m depth and analyzing the formation properties (including porosity) in detail [*Acworth et al.*, 2015].
3. Fowlers Gap, NSW, Australia (Piezometer 273282-2: latitude −31.065781°, longitude 141.762065°) where groundwater is confined by 75 m of consolidated clays [*Acworth et al.*, 2016]. A vented transducer (Level Troll 700H series, In-Situ Inc., USA) was used to monitor hydraulic heads, and atmospheric pressure was measured by an absolute gauge transducer (Vaisala, Finland). The piezometer was screened in clayey sands.

Earth tide gravitational time series data were synthesized using the software package TSoft (version 2.2.12 with a release date of 19 October 2015) [*Van Camp and Vauterin*, 2005] at the latitude, longitude, and elevation of the borehole at each site. The Earth tide was generated at the same sampling rate and duration as the pressure record for each location. We note that the Earth tide calculation is in UTC time and that other records require correction to this common time reference.

3. Results and Discussion

The time-frequency-amplitude content of the 12 year continuous Baldry atmospheric pressure record (Figure 1) was calculated by the application of WSST. It is clear that, while the 1 cpd frequency is subject to considerable seasonal variability [*Acworth and Brain*, 2008], the 2 cpd frequency component S_2^{AT} is remarkably constant and its amplitude more uniform.

Figure 2 shows a portion ($1.85 \leq f \leq 2.05$ cpd) of the amplitude spectrum of the synthesized Earth tide, atmospheric pressure, and the groundwater head for all three sites. Note that application of the FFT averages amplitudes and phases throughout the duration of the time record. The amplitudes for the M_2 and S_2 spectra and the phase difference between both S_2 drivers are presented in Table 1. Here equation 4 was used to calculate the respective aquifer BE. We further use estimates of aquifer porosity θ to quantify formation compressibility α as well as groundwater specific storage S_s.
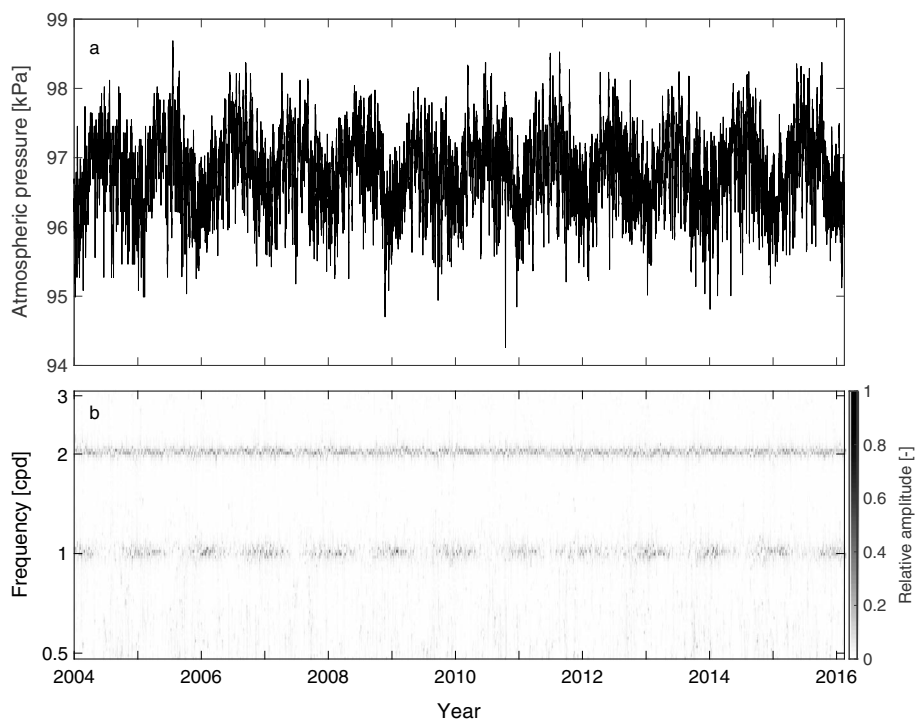
Figure 1. (a) Long-term (12 year) atmospheric pressure measured at Baldry and (b) the time-frequency amplitude in the range of 0.5 to 3 cpd calculated using the wavelet synchrosqueezed transform (WSST). Note the uniformity of the energy at 2 cpd compared to 1 cpd.

To illustrate our BE results, Figure 3 shows scatterplots where atmospheric pressure is plotted versus groundwater head. The correct slope of the correlation derived from the new method is shown for comparison.

The data for Fowlers Gap (Figure 3c) are closely grouped along a straight line. The Baldry data (Figure 3a) show portions of the data with a clear slope. However, as rainfall recharge and evapotranspiration play a significant part at this site [*Acworth and Brain*, 2008], there are many offsets away from the straight line. The Cattle Lane data (Figure 3b) show very little impact from atmospheric pressure variation, as indicated by the very low barometric efficiency (BE = 0.059) determined by the new method. Regardless, it would be difficult to reliably estimate a slope from the scatter cloud when BE is low or when groundwater head changes influence the correlation.

While Figure 2a illustrates the advantages of using a long data set, the length of continuous hydraulic head and barometric pressure records from the Baldry site (∼12 years) is by no means required for accurate BE calculations. A key consideration for time series lengths is the need to distinguish the amplitudes of the M_2 and S_2 components in the groundwater head data. The frequencies of these components differ by $\Delta f = 0.06773$ cpd, which establishes a theoretical minimum time series length of 14.76 days. Time series of at least double this length (i.e., ≳1 month) will allow for frequency samples between these two peaks which will aid in constraining their amplitudes. Following the *Nyquist-Shannon* sampling theorem, sampling rates > 4 cpd will enable signal frequencies ≥ 2 cpd to be resolved, although in practice a higher sampling rate is desirable to avoid aliasing from higher-frequency components and to allow for greater data quality control.

The proposed method has the following clear advantages:

1. Determination of a formation's BE value is relatively simple but accurate and robust against low BE values and hydraulic head changes.
2. The complete record is used to calculate the FFT and provides the basis for the method. No subjective choice of part of the record is required. For this reason, the BE results are both accurate and repeatable.
3. The gravitational Earth tides can be synthesized using TSoft [*Van Camp and Vauterin*, 2005] for any global time and location, provided that the geographic coordinates of the borehole are known.
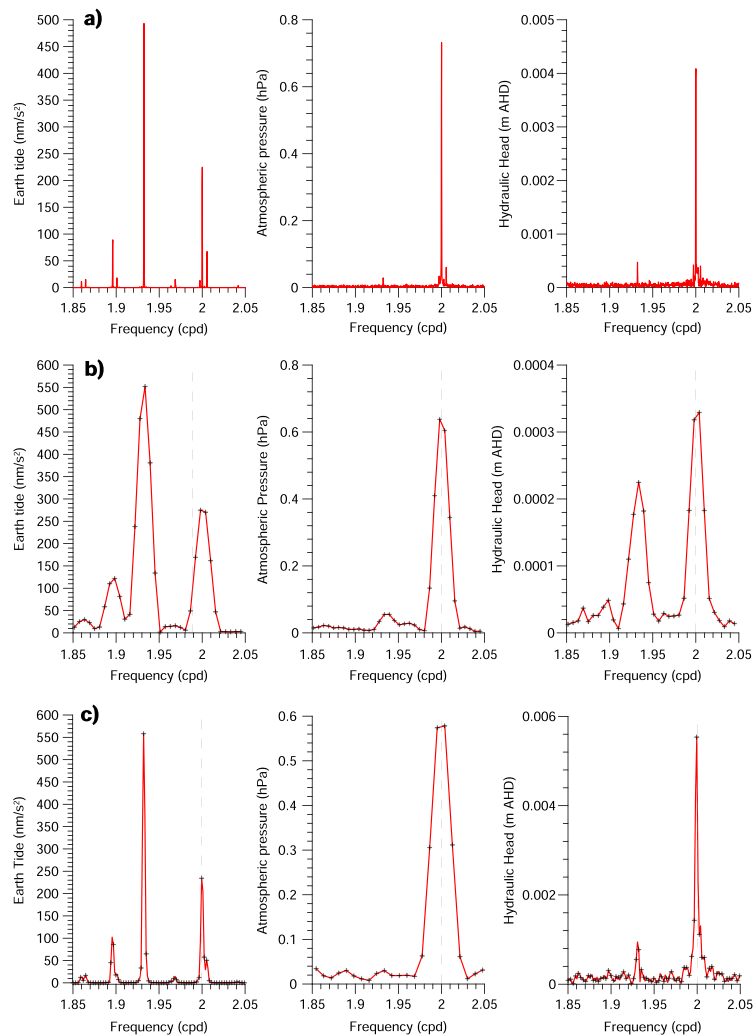
Figure 2. FFT amplitude spectra of Earth tide, atmospheric pressure, and groundwater head (left to right) in the range of 1.85 to 2.05 cpd for the locations (a) Baldry (BH1), (b) Cattle Lane (P35), and (c) Fowlers Gap (273282-2).

Table 1. Amplitudes of the M_2 and S_2 Components of the Earth Tide (ET), the Atmospheric Pressure (AT), and the Groundwater Head (GW) and Phase Differences ($\Delta\phi$) of the Earth Tide (ET) and the Atmospheric Pressure (AT) for the Three Field Sites[a]

				Field Site		
Component	Description	Parameter	Unit	Baldry	Cattle Lane	Fowlers Gap
M_2	Earth tide (synthesis)	M_2^{ET}	nm s^{-2}	492.526	551.572	558.075
	Hydraulic Head	M_2^{GW}	mm H$_2$O	0.471	0.225	0.773
S_2	Atmospheric pressure	S_2^{AT}	mm H$_2$O	7.461	6.164	5.897
	Earth tide (synthesis)	S_2^{ET}	nm s^{-2}	224.640	270.463	234.478
	Phase difference	$\Delta\phi$	°	−56.709	−71.726	-70.393
	Groundwater head	S_2^{GW}	mm H$_2$O	4.086	0.329	5.536
Barometric efficiency		**BE**	**-**	**0.563**	**0.059**	**0.976**
Porosity		ϕ	-	0.15	0.35	0.10
Formation compressibility		α	Pa^{-1}	5.332×10^{-11}	2.557×10^{-9}	1.126×10^{-12}
Specific storage		S_s	m^{-1}	2.094×10^{-6}	2.663×10^{-5}	1.586×10^{-6}

[a]Barometric efficiency BE is calculated using equation (4). Porosity is estimated for Baldry and Fowlers Gap but has been measured on core samples for Cattle Lane. Formation compressibility is calculated using equations (1) and (2), while specific storage is calculated using equation (3).
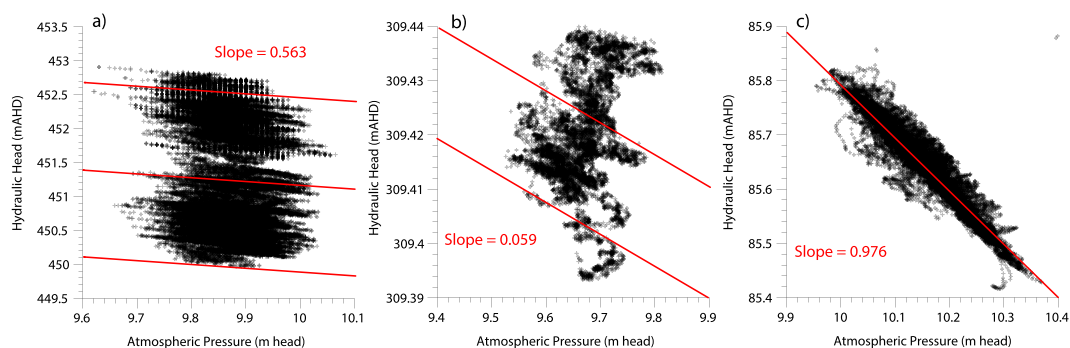
Figure 3. Scatterplots of atmospheric pressure versus groundwater heads for (a) Baldry, (b) Cattle Lane, and (c) Fowlers Gap. Slopes that are calculated from the new method (equation (4)) are included for comparison.

4. The presence of a BE > 0 in hydraulic heads is a strong indication that the groundwater at this location is confined. The ability to determine this from simple hydraulic head measurements without the need for further experiments is a clear advantage. For example, this can inform groundwater modeling where the assignment of unconfined or confined conditions determines the modeling approach.

5. The stability of the atmospheric tide at 2 cpd frequency relaxes the requirement for atmospheric and Earth tide records to exactly match in duration.

The following aspects require careful attention:

1. Performing FFT analysis requires that the data are regularly sampled with no data gaps in either the atmospheric pressure or the hydraulic head records.

2. All data sets need to be corrected to a common time reference (i.e., UTC) so that the phase difference between the Earth tide and the atmospheric tide can be accurately determined.

3. The use of vented transducers is recommended to minimize the risk of adding a phase change to the signal caused by lack of system clock synchronicity or time divergence.

4. It is important that the atmospheric pressure has not been corrected to sea level.

4. Implications for the Investigation of Groundwater Resources and Geotechnical Properties

The proposed method allows objective quantification of compressible groundwater storage properties using atmospheric tides by successfully removing the Earth tide influence. It makes use of the very uniform and ubiquitous atmospheric tide at 2 cpd to provide a source of energy. If the hydraulic head responds and is out of phase with the atmospheric driver by 180° (or π radians), then the subsurface is confined and its compressible storage properties can be quantified. The method overcomes significant shortcomings of previous approaches which are subjective and affected by changes of hydraulic heads (i.e., through natural or induced groundwater flow). The technique is truly in situ, accurate, and easy to implement.

The method only requires continuous barometric pressure and hydraulic head measurements sampled at least every 6 h over ≳ 1 month duration. Both of these parameters are part of standard data collection practice around the world, especially when using unvented pressure transducers. The method can therefore be applied to suitable existing records as no new field measurements are necessary. The only additional requirement is for the gravitational Earth tide which can be synthesized for any desired location, time, and duration with sufficient accuracy at this frequency.

Formation compressibility and groundwater specific storage can be derived, providing that porosity data are available. Alternatively, reasonable porosity estimates can establish probable maximal or minimal bounds for aquifer properties using less effort and providing higher accuracy compared to standard aquifer tests.

Using hydraulic head measurements from simply constructed piezometers screened at different depths, the proposed method can be applied through an aquifer/aquitard succession. These results can be incorporated into a multidimensional groundwater model to predict drawdown due to abstraction. The proposed method could, therefore, replace the use of expensive equipment to recover a minimally disturbed core for laboratory analysis. The method could facilitate improved evaluation of the potential for land subsidence caused

by groundwater extraction, which is a major global problem [*Alley et al.*, 2002; *Galloway and Burbey*, 2011], especially in coastal areas [*Higgins et al.*, 2013].

References

Acworth, R. I., and T. Brain (2008), Calculation of barometric efficiency in shallow piezometers using water levels, atmospheric and Earth tide data, *Hydrogeol. J.*, *16*(8), 1469–1481, doi:10.1007/s10040-008-0333-y.

Acworth, R. I., W. Timms, B. Kelly, D. McGeeney, T. Ralph, Z. Larkin, and R. GC (2015), Late Cenozoic paleovalley fill sequence from the Southern Liverpool Plains, New South Wales—Implications for groundwater resource evaluation, *Aust. J. Earth Sci.*, *62*(6), 1–24, doi:10.1080/08120099.2015.1086815.

Acworth, R. I., G. C. Rau, M. O. Cuthbert, E. Jensen, and K. Leggett (2016), Long-term spatio-temporal precipitation variability in arid-zone Australia and implications for groundwater recharge, *Hydrogeol. J.*, *24*(4), 905–921, doi:10.1007/s10040-015-1358-7.

Alley, W. M., R. W. Healy, J. W. LaBaugh, and T. E. Reilly (2002), Flow and storage in groundwater systems, *Science*, *296*(5575), 1985–1990, doi:10.1126/science.1067123.

Briciu, A.-E. (2014), Wavelet analysis of lunar semidiurnal tidal influence on selected inland rivers across the globe, *Sci. Rep.*, *4*, 4193, doi:10.1038/srep04193.

Cartwright, D. E. (1999), *Tides: A Scientific History*, Cambridge Univ. Press, Cambridge, U. K.

Cooper, H. H. (1966), The equation of groundwater flow in fixed and deforming coordinates, *J. Geophys. Res.*, *71*(20), 4785–4790, doi:10.1029/JZ071i020p04785.

Cutillo, P. A., and J. D. Bredehoeft (2011), Estimating aquifer properties from the water level response to Earth tides, *Ground Water*, *49*(4), 600–610, doi:10.1111/j.1745-6584.2010.00778.x.

Daubechies, I., J. Lu, and H.-T. Wu (2011), Synchrosqueezed wavelet transforms: An empirical mode decomposition-like tool, *Appl. Comput. Harmon. Anal.*, *30*(2), 243–261, doi:10.1016/j.acha.2010.08.002.

Domenico, P. A., and F. W. Schwartz (1997), *Physical and Chemical Hydrogeology*, 2nd ed., 528 pp., John Wiley, New York.

Galloway, D. L., and T. J. Burbey (2011), Review: Regional land subsidence accompanying groundwater extraction, *Hydrogeol. J.*, *19*(8), 1459–1486, doi:10.1007/s10040-011-0775-5.

Gonthier, G. J. (2007), A graphical method for estimation of barometric efficiency from continuous data-concepts and application to a site in the Piedmont, Air Force Plant 6, Marietta, Georgia, *Tech. Rep. 2007-5111*, U. S. Geol. Surv., Reston, Va.

Harris, F. (1978), On the use of windows for harmonic analysis with the discrete Fourier transform, *Proc. IEEE*, *66*(1), 51–83, doi:10.1109/PROC.1978.10837.

Higgins, S., I. Overeem, A. Tanaka, and J. P. M. Syvitski (2013), Land subsidence at aquaculture facilities in the Yellow River delta, China, *Geophys. Res. Lett.*, *40*, 3898–3902, doi:10.1002/grl.50758.

Hsieh, P. A., J. D. Bredehoeft, and J. M. Farr (1987), Determination of aquifer transmissivity from Earth tide analysis, *Water Resour. Res.*, *23*(10), 1824–1832, doi:10.1029/WR023i010p01824.

Jacob, C. E. (1940), On the flow of water in an elastic artesian aquifer, *Eos Trans. AGU*, *21*(2), 574–586, doi:10.1029/TR021i002p00574.

Merritt, M. L. (2004), Estimating hydraulic properties of the Floridan aquifer system by analysis of Earth-tide, ocean-tide, and barometric effects, Collier and Hendry Counties, Florida, *Tech. Rep. 4267*, U. S. Geol. Surv., Reston, Va.

Palumbo, A. (1998), Atmospheric tides, *J. Atmos. Sol. Terr. Phys.*, *60*(3), 279–287, doi:10.1016/S1364-6826(97)00078-3.

Rojstaczer, S. (1988), Determination of fluid flow properties from the response of water levels in wells to atmospheric loading, *Water Resour. Res.*, *24*(11), 1927–1938, doi:10.1029/WR024i011p01927.

Rojstaczer, S., and D. C. Agnew (1989), The influence of formation material properties on the response of water levels in wells to Earth tides and atmospheric loading, *J. Geophys. Res.*, *94*(B9), 12,403–12,411, doi:10.1029/JB094iB09p12403.

Thakur, G., E. Brevdo, N. S. Fučkar, and H.-T. Wu (2013), The synchrosqueezing algorithm for time-varying spectral analysis: Robustness properties and new paleoclimate applications, *Sig. Proc.*, *93*(5), 1079–1094, doi:10.1016/j.sigpro.2012.11.029.

Van Camp, M., and P. Vauterin (2005), Tsoft: Graphical and interactive software for the analysis of time series and Earth tides, *Comput. Geosci.*, *31*(5), 631–640, doi:10.1016/j.cageo.2004.11.015.

Van Der Kamp, G., and J. E. Gale (1983), Theory of Earth tide and barometric effects in porous formations with compressible grains, *Water Resour. Res.*, *19*(2), 538–544, doi:10.1029/WR019i002p00538.

Wada, Y., L. P. H. Van Beek, C. M. Van Kempen, J. W. T. M. Reckman, S. Vasak, and M. F. P. Bierkens (2010), Global depletion of groundwater resources, *Geophys. Res. Lett.*, *37*, L20402, doi:10.1029/2010GL044571.